

# The rotational spectrum of the CH radical in its $a^4\Sigma^-$ state, studied by far-infrared laser magnetic resonance

Thomas Nelis<sup>a)</sup> and John M. Brown

Physical Chemistry Laboratory, South Parks Road, Oxford, OX1 3QZ, England

Kenneth M. Evenson

Time and Frequency Division, National Institute of Standards and Technology, Boulder, Colorado 80303

(Received 20 October 1989; accepted 12 December 1989)

The CH radical has been detected in its  $a^4\Sigma^-$  state by the technique of laser magnetic resonance at far-infrared wavelengths. Spectra relating to different spin components of the first three rotational transitions have been recorded. The molecule was generated either by the reaction of F atoms with  $\text{CH}_4$ , with a trace of added oxygen or by the reaction of O atoms with  $\text{C}_2\text{H}_2$ . The observed resonances have been analyzed and fitted to determine the parameters of an effective Hamiltonian for a molecule in a  $^4\Sigma$  state. The principal quantities determined are the rotational constant  $B_0 = 451\,138.434(94)$  MHz and the spin-spin parameter  $\lambda_0 = 2785.83(18)$  MHz. Proton hyperfine parameters have also been determined.

## I. INTRODUCTION

The CH-free radical is a highly reactive species which plays a part in a great variety of gas phase chemical reactions. It has long been appreciated that CH is present in many hydrocarbon flames and combustion processes<sup>1</sup> and it is thought to be the main source of chemions in hydrocarbon flames.<sup>2</sup> It also occurs in a number of extraterrestrial sources. For example, it is a well-known constituent of the solar spectrum<sup>3</sup> and a few years ago it was also identified in the interstellar medium.<sup>4,5</sup>

The identification of CH in these different environments usually relied on spectroscopic observation. Its electronic spectrum was detected in 1918<sup>6</sup> and played an important part in the development of our understanding of the energy levels of diatomic molecules.<sup>7-9</sup> Since then, the electronic spectrum has been studied extensively and the vibration-rotation levels of many electronic states are now known.<sup>10,11</sup> Pure rotational transitions in CH in its ground state were detected by far-infrared laser magnetic resonance (LMR)<sup>12</sup> and analyzed to give much more precise molecular parameters.<sup>13,14</sup> Very recently, the same transitions have been detected in a tunable far-infrared experiment.<sup>15</sup> The lambda-doubling spectrum of CH falls in the microwave region and was first detected by radioastronomers.<sup>4,5</sup> These observations have been extended by laboratory microwave work.<sup>16,17</sup> Finally, the vibration-rotation of CH in the  $X^2\Pi$  state has been recorded, using a difference frequency laser spectrometer.<sup>18</sup> However, despite this wealth of information, transitions between quartet states of the molecule had not been reported until we published our preliminary communication on the detection of spectroscopic transitions involving the quartet states of the molecule.<sup>19</sup>

The lowest quartet state of CH is the  $a^4\Sigma^-$  state, which arises from the first excited configuration ( $1\sigma^2 2\sigma^2 3\sigma^1 1\pi^2$ ). *Ab initio* calculations suggest that this state is very low lying, only  $0.63 \pm 0.12$  eV above the ground state.<sup>20,21</sup> This value is consistent with the value of  $0.742 \pm 0.008$  eV determined by

Kasdan, Herbst, and Lineberger<sup>22</sup> in the photoelectron spectrum of  $\text{CH}^-$ . However, because of the small effect of spin-orbit coupling, the  $a^4\Sigma^-$  state is metastable and no direct electronic transition into this state has yet been observed. We previously reported the observation of the pure rotational spectrum of CH in  $v=0$  level of the  $a^4\Sigma^-$  state by far-infrared LMR.<sup>19</sup> In this paper, we describe the detection of additional transitions and present a full analysis in terms of an effective Hamiltonian. The implications for the structure of CH in its  $a^4\Sigma^-$  state are also discussed. It is hoped that this work will stimulate further spectroscopic studies of the molecule and illuminate the role which it plays in chemistry.

## II. EXPERIMENTAL DETAILS

The far-infrared LMR spectra of CH in its  $a^4\Sigma^-$  state were recorded at the Boulder laboratories of the National Institute of Standards and Technology using a spectrometer which has been described in detail elsewhere.<sup>23</sup> The CH radicals were formed in the spectrometer sample volume by the reaction of fluorine atoms with methane in a flow system, the fluorine atoms being generated by passing a 5% mixture of fluorine in helium through a microwave discharge. The addition of a trace of oxygen to the He/ $\text{F}_2$  mixture increased the signal by a factor of about 2. A similar improvement in signal on addition of oxygen was observed for CH in its  $X^2\Pi$  state also. By reducing the total pressure in the sample region to about 200 mTorr (26 Pa), it was possible to observe Lamb dips on the strongest signals. As described in our earlier paper,<sup>19</sup> it was also possible to generate CH in its  $a^4\Sigma^-$  state in comparable concentrations by the reaction of oxygen atoms with acetylene. However, this alternative reaction produced several other free radical species whose LMR signals obscured those of CH in places so it was not used for measurement purposes. Magnetic flux densities were measured by a rotating coil probe which was calibrated periodically against a proton NMR gaussmeter. The uncertainty in the flux measurements is  $10^{-5}$  T below 0.1 T and  $10^{-4}$   $B_0$  above 0.1 T, where  $B_0$  is the magnetic flux density.

The observed far-infrared LMR spectrum of the CH

<sup>a)</sup> Visitor from the Institute of Applied Physics, University of Bonn, Wege-lerstrasse 8, D5300 Bonn 1, West Germany.

radical in the  $v = 0$  level of the  $a^4\Sigma^-$  state is summarized in Table I. The rotational transitions involved the first four rotational levels and are shown in the energy level diagram of Fig. 1. The details of the seven laser lines used in our work are also given in Table I. The frequencies are taken for the most part from the review of Inguscio *et al.*<sup>24</sup> Two of the frequencies were measured especially for this work and were first reported in our earlier paper.<sup>19</sup> The uncertainty in the laser frequency arises mainly from reproducibility in setting the laser to the peak of the gain profile. This uncertainty is about  $2 \times 10^{-7}$  of the laser frequency.

Examples of the spectra are shown in Figs. 2 and 3. Figure 2 shows the spectrum recorded with the  $332.1 \mu\text{m}$  laser line of  $\text{CH}_3\text{OD}$  with the electric vector of the far-infrared radiation perpendicular to the applied magnetic field ( $\sigma$  polarization). The doublet structure for each Zeeman component arises from the proton hyperfine interaction. This splitting of about 4 mT is observed for all transitions. Figure 3 shows the spectrum recorded with the  $166.6 \mu\text{m}$  line of  $\text{CH}_2\text{F}_2$ , this time in parallel (or  $\pi$ ) polarization. At low pressures it was possible to record Lamb dips on the strongest lines; an example of a proton hyperfine doublet taken from the  $166.6 \mu\text{m}$  spectrum is shown in Fig. 4. No spectra which could be attributed to CH in an excited vibrational level of the  $a^4\Sigma^-$  state have been observed with the laser lines given in Table I. The rotational constant  $B$  is expected to show quite a strong dependence on vibrational quantum number<sup>20</sup> so that the rotational transitions for  $v > 0$  corresponding to those in Table I occur at significantly lower frequencies.

### III. THEORETICAL MODEL

Previous work on the LMR spectra of a variety of molecules<sup>14,23,25</sup> has suggested that it should be possible to analyze an extensive body of magnetic resonance data such as the present in terms of a single model using a suitably constructed effective Hamiltonian. The model is fitted to the data by adjusting its parameters such as rotational constant, fine structure parameters and  $g$  factors so as to minimize the sum of the squares of the residuals. The form of the effective Hamiltonian for a molecule in a  $4\Sigma^-$  state has been discussed by several authors.<sup>26-28</sup> Drawing on these results, we write

$$H_{\text{eff}} = H_{\text{rot}} + H_{\text{ss}} + H_{\text{sr}} + H_{\text{hfs}} + H_z, \quad (1)$$

TABLE I. Summary of transitions observed in CH in the  $v = 0$  level of the  $a^4\Sigma^-$  state by LMR.

Transition $N' - N''$	$\lambda / \mu\text{m}$	Laser line $\nu / \text{MHz}^a$	Lasing gas	$\text{CO}_2$ pump
1-0	333.3	899 571.7	$^{13}\text{CD}_3\text{OD}$	10P16
	332.1	902 630.2	$\text{CH}_3\text{OD}$	9R4
	331.7	903 889.4	$\text{N}_2\text{H}_4$	9P12
	331.3	904 899.5 <sup>b</sup>	$\text{N}_2\text{H}_4$	9P12
2-1	166.7	1 798 647.0	$\text{CH}_2\text{F}_2$	9R22
	166.6	1 799 139.3	$\text{CH}_2\text{F}_2$	9R20
3-2	110.7	2 707 749.3	$\text{CH}_3\text{OH}$	9P36

<sup>a</sup>Laser frequencies given in Ref. 24.

<sup>b</sup>Laser frequency reported incorrectly in Ref. 19.

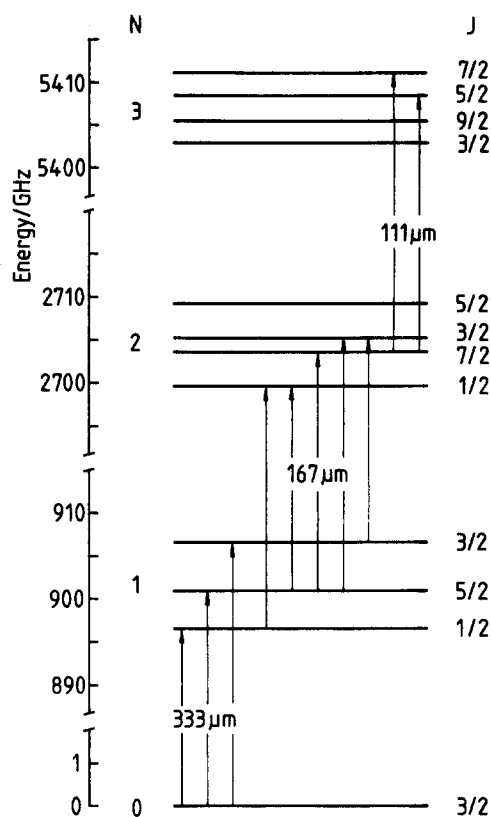


FIG. 1. Energy level diagram showing the transitions observed between the four lowest rotational levels of CH in the  $v = 0$  level of the  $a^4\Sigma^-$  state. The full details of the laser lines employed are given in Table I.

where  $H_{\text{rot}}$  represents the rotational kinetic energy including centrifugal distortion,  $H_{\text{ss}}$  is the electron spin dipole-dipole coupling term,  $H_{\text{sr}}$  is the spin-rotation interaction,  $H_{\text{hfs}}$  represents the nuclear spin hyperfine interaction and  $H_z$  represents the Zeeman effect of the applied magnetic field. The explicit forms of the various terms are as follows:

$$H_{\text{rot}} = BN^2 - DN^4 + HN^6, \quad (2)$$

$$H_{\text{ss}} = \frac{2}{3}\sqrt{6}\lambda T_{q=0}^2(\text{S,S}) + \frac{1}{3}\sqrt{6}\lambda_D [T_{q=0}^2(\text{S,S}), N^2]_+, \quad (3)$$

$$H_{\text{sr}} = \gamma\mathbf{N}\cdot\mathbf{S} + \gamma_D(\mathbf{N}\cdot\mathbf{S})N^2 + CT^3(\mathbf{L}^2, \mathbf{N})\cdot T^3(\text{S,S,S}), \quad (4)$$

$$H_{\text{hfs}} = b_F\mathbf{I}\cdot\mathbf{S} + \frac{1}{3}c\sqrt{6}T_{q=0}^2(\text{I,S}), \quad (5)$$

$$H_z = g_S\mu_B B_0 T_{p=0}^1(\text{S}) - g_r\mu_B B_0 T_{p=0}^1(\text{N}). \quad (6)$$

Where expedient, we have utilized standard spherical tensor notation<sup>29</sup> with  $p$  referring to laboratory-fixed components and  $q$  to molecule-fixed components. In line with our previous work, we have formulated the rotationally dependent operators in terms of  $\mathbf{N}^2 = (\mathbf{J} - \mathbf{S})^2$  rather than  $\mathbf{R}^2$  (this difference is unimportant for molecules in  $\Sigma$  states<sup>30</sup>). All the terms given above are quite standard apart from the third term in Eq. (4). This is a new, more compact description of the third order spin-orbit coupling effects first discussed by Hougen<sup>26</sup> and explored in more detail by Brown and Milton.<sup>27</sup> The advantage of the present formulation is that it makes explicit the third rank dependence on the total spin operator  $\mathbf{S}$ ; it is thus immediately obvious that such effects will only manifest themselves in states of quartet or higher

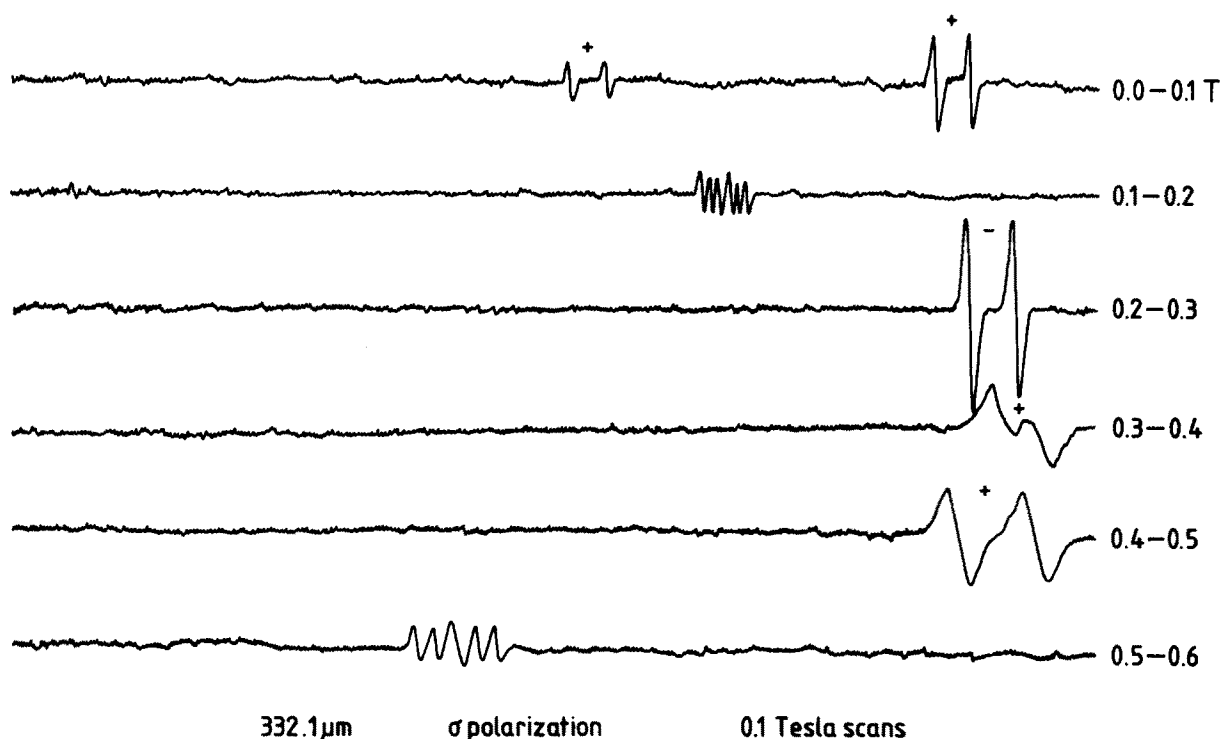


FIG. 2. Survey spectrum of the CH radical in the  $a^4\Sigma^-$  state recorded in perpendicular polarization ( $\Delta M_J = \pm 1$ ) with the  $332.1 \mu\text{m}$  laser line of  $\text{CH}_3\text{OD}$ . The spectrum is associated with all three fine structure components of the  $N = 1-0$  rotational transition. The proton hyperfine doubling can be clearly seen for each Zeeman component. The + or - signs give the experimentally determined signs of the tuning rates  $\partial\nu/\partial B_0$  for each transition. The two doublets of triplets arise from NH in the  $X^3\Sigma^-$  state, which was present as an impurity. The quantum number assignments for this spectrum can be deduced from the calculated frequency/field dependence shown in Fig. 6.

multiplicity. Furthermore, the form is more general than the previous treatment, since it is not restricted to a particular multiplicity or coupling scheme. The parameter  $C$  can be related to  $\gamma_S$  used by earlier workers:

$$C \langle \Lambda | T_{q=0}^2(L^2) | \Lambda \rangle = (10/\sqrt{6})\gamma_S. \quad (7)$$

The most appropriate basis set for molecules in  $\Sigma$  states

is usually Hund's case (b).<sup>31</sup> This is certainly the case for the  $a^4\Sigma^-$  state of CH, for which the rotational constant is large and the fine structure comparatively small. In an external magnetic field, the nuclear spin  $I$  tends to precess around the applied field rather than being coupled to the total molecular angular momentum  $J$  to give a grand total angular momentum  $F$ . Therefore the  $I$ -decoupled basis set  $|N, S, J, M_J, I, M_I\rangle$

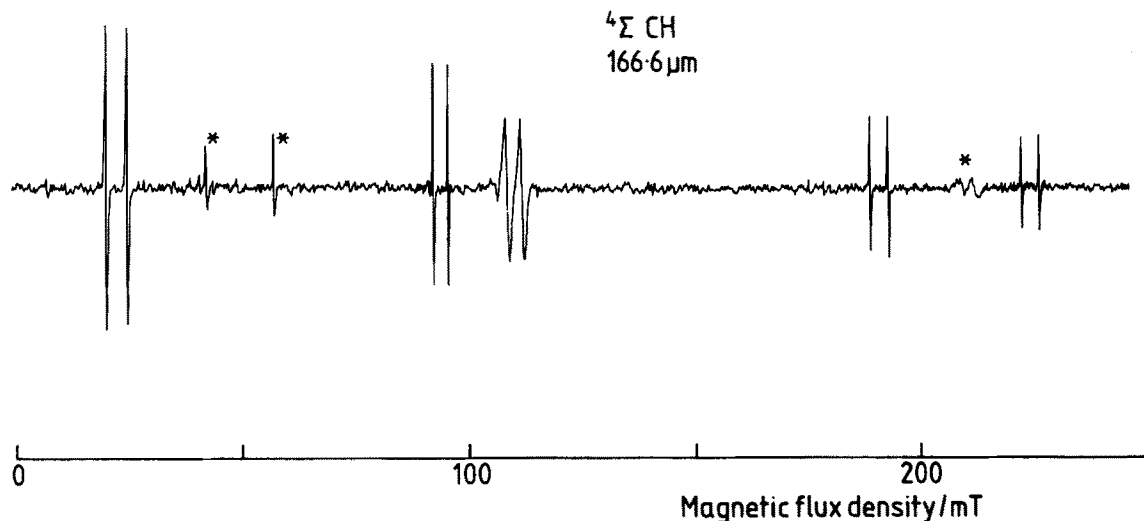


FIG. 3. Survey spectrum of the CH radical in the  $a^4\Sigma^-$  state recorded in parallel polarization ( $\Delta M_J = 0$ ) with the  $166.6 \mu\text{m}$  laser line of  $\text{CH}_2\text{F}_2$ . The rotational transition is  $N = 2-1$ : several different fine structure transitions are involved, see Fig. 7. The lines marked with asterisks arise from unidentified impurities. Note the very obvious proton hyperfine doublet structure.

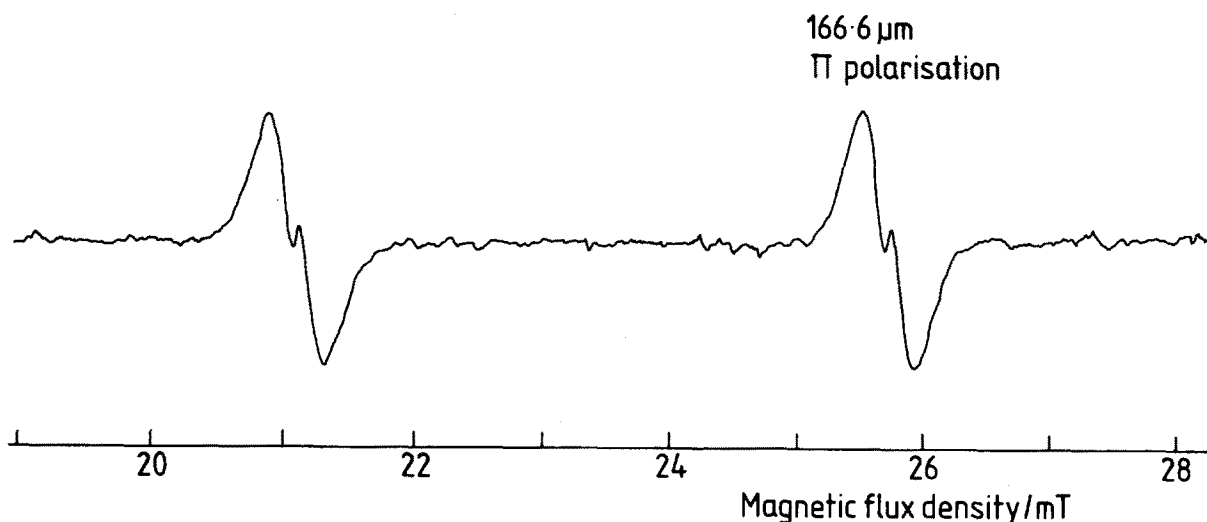


FIG. 4. Examples of Lamb dips recorded in the LMR spectrum of CH in its  $a^4\Sigma^-$  state, taken in this case from the  $166.6\ \mu\text{m}$  spectrum in parallel polarization (see Fig. 3). The total pressure was 220 mTorr (29 Pa).

is used in the present work. The problem of labeling the eigenstates involved in the LMR experiment is particularly acute. None of the quantum numbers  $M_S, M_N, M_J, M_I, J$ , or  $F$  remains good over the complete field range used in our experiments (0–1 T). The simplest solution is to number the different eigenstates in order of increasing energy but this is at the expense of all physical insight. It is more illuminating to try to use at least some of the quantum numbers (in addition to  $M_F$ ). We have therefore characterized each state for the molecule in a small magnetic flux density (50 mT) and used the quantum numbers which are well defined there ( $J, M_J, M_I$ ) to label the state under all other conditions. This

scheme works well, failing only when avoided level crossings occur. An example of such an avoided crossing in the rotational level  $N = 1$  for CH is described in the next section.

The eigenvalues of a molecule in a  $^4\Sigma$  state were computed by numerical diagonalization of the effective Hamiltonian in Eq. (1), expressed in a Hund's case (b) basis set. Almost all the terms in this Hamiltonian are quite standard and their matrix elements have been given several times before, see, e.g., Ref. 28. The one exception is the third order correction to the spin-rotation interaction ( $\gamma_S$ ) given in Eqs. (4) and (7). Expressed in standard spherical tensor notation, the matrix elements of this operator in a case (b) basis set are

$$\begin{aligned} & \langle N' \Lambda' S' J' M_J' | H_{sr}^{(3)} | N \Lambda S J M_J \rangle \\ &= \delta_{J'J} \delta_{M_J' M_J} \gamma_S (\sqrt{70/4\sqrt{6}}) (-)^{N+S+J+1} \\ & \times \begin{Bmatrix} J & S & N' \\ 3 & N & S \end{Bmatrix} (-)^{N+N'} \begin{Bmatrix} 2 & 1 & 3 \\ N & N' & N \end{Bmatrix} [(2N'+1)(2N+1)]^{1/2} (-)^{N'-\Lambda} \\ & \times \begin{pmatrix} N' & 2 & N \\ -\Lambda & 0 & \Lambda \end{pmatrix} [N(N+1)(2N+1)]^{1/2} [(2S-2)(2S-1)(2S)(2S+1)(2S+2)(2S+3)(2S+4)]^{1/2}. \quad (8) \end{aligned}$$

This expression is general and in a convenient form for coding in a computer program. For a  $2S+1\Sigma$  state with  $\Lambda = 0$ , only matrix elements with  $\Delta N = 0, \pm 2$  are nonzero. The explicit forms of these elements are given in the appendix, along with the matrix elements of a complete effective Hamiltonian for a  $^4\Sigma$  state. It should be stressed that this new form of the third order spin-rotation term is equivalent to the original version given by Brown and Milton<sup>27</sup> who chose to work in a case (a) basis set. The off-diagonal elements of the operator in Eq. (4), when expressed in such a basis set, are identical to those of Brown and Milton. However, it also generates diagonal matrix elements in a case (a) basis set, terms which were ignored by Brown and Milton.

#### IV. RESULTS AND ANALYSIS

The detailed measurements of the resonances associated with CH in the  $\nu = 0$  level of the  $a^4\Sigma^-$  state are given in Table II, along with the quantum number assignments.

The analysis was far from trivial and the assignments were arrived at only after a lengthy process of trial and error. The difficulty in the analysis stemmed from two causes. First, at the start of our work there was a dearth of knowledge of the properties of CH in any of its quartet states. Secondly, the Zeeman effects displayed by the molecule are highly nonlinear because the electron spin is easily decoupled from the molecular framework by the magnetic field, a

TABLE II. Measurements and assignments of flux densities and frequencies of transitions observed by far-infrared LMR for CH in the  $\alpha^4\Sigma^-$  state.

$J$	$M_J$	$M_I^a$	Flux density (mT)	(obs-calc)		Rel. intensity <sup>b</sup>	$\partial\nu/\partial B_0^b$ MHz/mT
					MHz		
333.3 $\mu\text{m}$ spectrum $\nu_L = 899\,571.7$ MHz $N = 1 \leftarrow 0$							
polarization ( $\pi$ )							
$2\frac{1}{2} \leftarrow 1\frac{1}{2}$	$1\frac{1}{2} \leftarrow 1\frac{1}{2}$	$\frac{1}{2}$	71.9	-0.9		0.082	-21.0
	$1\frac{1}{2} \leftarrow 1\frac{1}{2}$	$-\frac{1}{2}$	76.4	-0.8		0.082	-21.1
$2\frac{1}{2} \leftarrow 1\frac{1}{2}$	$\frac{1}{2} \leftarrow \frac{1}{2}$	$\frac{1}{2}$	156.00 <sup>d</sup>	0.2		0.257	-6.0
	$\frac{1}{2} \leftarrow \frac{1}{2}$	$-\frac{1}{2}$	161.47 <sup>d</sup>	0.5		0.258	-5.9
⊥ polarization ( $\sigma$ )							
$\frac{1}{2} \leftarrow 1\frac{1}{2}$	$\frac{1}{2} \leftarrow -\frac{1}{2}$	$\frac{1}{2}$	90.7	3.0		0.125	26.9
	$\frac{1}{2} \leftarrow -\frac{1}{2}$	$-\frac{1}{2}$	94.8	3.8		0.126	26.9
$2\frac{1}{2} \leftarrow 1\frac{1}{2}$	$-1\frac{1}{2} \leftarrow -\frac{1}{2}$	$\frac{1}{2}$	95.0	-1.6		0.119	-18.0
	$-1\frac{1}{2} \leftarrow -\frac{1}{2}$	$-\frac{1}{2}$	98.7	-1.4		0.120	-17.9
$\frac{1}{2} \leftarrow 1\frac{1}{2}$	$-\frac{1}{2} \leftarrow -1\frac{1}{2}$	$\frac{1}{2}$	332.15 <sup>d</sup>	0.3		0.301	3.5
	$-\frac{1}{2} \leftarrow -1\frac{1}{2}$	$-\frac{1}{2}$	340.45 <sup>d</sup>	0.0		0.302	3.4
332.1 $\mu\text{m}$ spectrum $\nu_L = 902\,630.2$ MHz $N = 1 \leftarrow 0$							
polarization ( $\pi$ )							
$2\frac{1}{2} \leftarrow 1\frac{1}{2}$	$-1\frac{1}{2} \leftarrow -1\frac{1}{2}$	$\frac{1}{2}$	134.03 <sup>d</sup>	-1.0		0.241	7.8
	$-1\frac{1}{2} \leftarrow -1\frac{1}{2}$	$-\frac{1}{2}$	137.30 <sup>d</sup>	-1.2		0.240	7.9
⊥ polarization ( $\sigma$ )							
$2\frac{1}{2} \leftarrow 1\frac{1}{2}$	$-\frac{1}{2} \leftarrow -1\frac{1}{2}$	$\frac{1}{2}$	51.1	1.7		0.050	28.8
		$-\frac{1}{2}$	54.5	1.6		0.049	28.7
$2\frac{1}{2} \leftarrow 1\frac{1}{2}$	$\frac{1}{2} \leftarrow -\frac{1}{2}$	$\frac{1}{2}$	84.88 <sup>d</sup>	-0.4		0.130	17.3
		$-\frac{1}{2}$	88.13 <sup>d</sup>	-0.8		0.130	17.3
$1\frac{1}{2} \leftarrow 1\frac{1}{2}$	$\frac{1}{2} \leftarrow 1\frac{1}{2}$	$\frac{1}{2}$	288.40 <sup>d</sup>	0.3		0.296	-4.6
		$-\frac{1}{2}$	292.79 <sup>d</sup>	0.5		0.297	-4.6
$2\frac{1}{2} \leftarrow 1\frac{1}{2}$	$1\frac{1}{2} \leftarrow \frac{1}{2}$	$-\frac{1}{2}$	388.29 <sup>d</sup>	2.5		0.318	1.3
		$\frac{1}{2}$	391.62 <sup>d</sup>	1.9		0.319	1.2
$\frac{1}{2} \leftarrow 1\frac{1}{2}$	$\frac{1}{2} \leftarrow -\frac{1}{2}$	$\frac{1}{2}$	487.11 <sup>d</sup>	-1.6		0.325	1.3
		$-\frac{1}{2}$	494.25 <sup>d</sup>	-1.6		0.325	1.3
331.7 $\mu\text{m}$ spectrum $\nu_L = 903\,889.4$ MHz $N = 1 \leftarrow 0$							
⊥ polarization ( $\sigma$ )							
$2\frac{1}{2} \leftarrow 1\frac{1}{2}$	$-\frac{1}{2} \leftarrow -1\frac{1}{2}$	$\frac{1}{2}$	97.0	3.6		0.052	26.4
	$-\frac{1}{2} \leftarrow -1\frac{1}{2}$	$-\frac{1}{2}$	100.4	3.7		0.052	26.4
$1\frac{1}{2} \leftarrow 1\frac{1}{2}$	$\frac{1}{2} \leftarrow 1\frac{1}{2}$	$\frac{1}{2}$	125.4	-2.0		0.242	-12.6
	$\frac{1}{2} \leftarrow 1\frac{1}{2}$	$-\frac{1}{2}$	129.1	-2.0		0.243	-12.6
$2\frac{1}{2} \leftarrow 1\frac{1}{2}$	$\frac{1}{2} \leftarrow -\frac{1}{2}$	$\frac{1}{2}$	151.0	5.6		0.078	21.5
	$\frac{1}{2} \leftarrow -\frac{1}{2}$	$-\frac{1}{2}$	154.4	4.7		0.079	21.5
$1\frac{1}{2} \leftarrow 1\frac{1}{2}$	$-\frac{1}{2} \leftarrow \frac{1}{2}$	$\frac{1}{2}$	353.7	0.7		0.323	-1.7
	$-\frac{1}{2} \leftarrow \frac{1}{2}$	$-\frac{1}{2}$	360.7	1.2		0.323	-1.6
$1\frac{1}{2} \leftarrow 1\frac{1}{2}$	$-1\frac{1}{2} \leftarrow -\frac{1}{2}$	$\frac{1}{2}$	411.0	0.8		0.314	-1.6
	$-1\frac{1}{2} \leftarrow -\frac{1}{2}$	$-\frac{1}{2}$	417.4	1.0		0.314	-1.6
331.3 $\mu\text{m}$ spectrum $\nu_L = 904\,899.5$ MHz $N = 1 \leftarrow 0$							
polarization ( $\pi$ )							
$1\frac{1}{2} \leftarrow 1\frac{1}{2}$	$1\frac{1}{2} \leftarrow 1\frac{1}{2}$	$-\frac{1}{2}$	403.42 <sup>d</sup>	-0.1		0.318	-1.2
	$1\frac{1}{2} \leftarrow 1\frac{1}{2}$	$\frac{1}{2}$	424.33 <sup>d</sup>	0.9		0.320	-1.1
⊥ polarization ( $\sigma$ )							
$1\frac{1}{2} \leftarrow 1\frac{1}{2}$	$\frac{1}{2} \leftarrow 1\frac{1}{2}$	$\frac{1}{2}$	62.6	-2.2		0.196	-20.2
	$\frac{1}{2} \leftarrow 1\frac{1}{2}$	$-\frac{1}{2}$	66.4	-1.8		0.198	-20.3
$1\frac{1}{2} \leftarrow 1\frac{1}{2}$	$-\frac{1}{2} \leftarrow \frac{1}{2}$	$\frac{1}{2}$	103.4	-0.1		0.275	-9.3
	$-\frac{1}{2} \leftarrow \frac{1}{2}$	$-\frac{1}{2}$	108.0	-0.3		0.275	-9.2
$1\frac{1}{2} \leftarrow 1\frac{1}{2}$	$-1\frac{1}{2} \leftarrow -\frac{1}{2}$	$\frac{1}{2}$	135.8	0.2		0.242	-7.7
	$-1\frac{1}{2} \leftarrow -\frac{1}{2}$	$-\frac{1}{2}$	141.4	-0.2		0.242	-7.7
166.7 $\mu\text{m}$ spectrum $\nu_L = 1\,798\,647.0$ MHz $N = 2 \leftarrow 1$							
polarization ( $\pi$ )							
$1\frac{1}{2} \leftarrow 1\frac{1}{2}$	$1\frac{1}{2} \leftarrow 1\frac{1}{2}$	$\frac{1}{2}$	0.0	3.8		0.124	-23.0
	$\frac{1}{2} \leftarrow \frac{1}{2}$	$\frac{1}{2}$	7.3	1.0		0.032	-14.3
	$1\frac{1}{2} \leftarrow \frac{1}{2}$	$-\frac{1}{2} \leftarrow \frac{1}{2}$	12.1	5.0		0.007	-11.5
$\frac{1}{2} \leftarrow \frac{1}{2}$	$\frac{1}{2} \leftarrow \frac{1}{2}$	$\frac{1}{2}$	104.3	-5.9		0.051	-42.5
	$\frac{1}{2} \leftarrow \frac{1}{2}$	$-\frac{1}{2}$	107.6	-5.5		0.051	-42.5
$3\frac{1}{2} \leftarrow 2\frac{1}{2}$	$2\frac{1}{2} \leftarrow 2\frac{1}{2}$	$\frac{1}{2}$	212.2	-6.1		0.031	-23.6
	$2\frac{1}{2} \leftarrow 2\frac{1}{2}$	$-\frac{1}{2}$	216.2	-5.5		0.031	-23.6
	$\frac{1}{2} \leftarrow \frac{1}{2}$	$\frac{1}{2}$	242.6	-7.5		0.017	-28.0
	$\frac{1}{2} \leftarrow \frac{1}{2}$	$-\frac{1}{2}$	246.6	-6.8		0.017	-28.0

TABLE II (continued).

l polarization ( $\sigma$ )							
$1\frac{1}{2} \leftarrow 1\frac{1}{2}$	$\frac{1}{2} \leftarrow 1\frac{1}{2}$	$-\frac{1}{2}$	0.0	3.7	0.093	-15.7	
	$-\frac{1}{2} \leftarrow \frac{1}{2}$	$\frac{1}{2}$	4.9	0.7	0.099	-22.7	
$1\frac{1}{2} \leftarrow 1\frac{1}{2}$	$1\frac{1}{2} \leftarrow \frac{1}{2}$	$-\frac{1}{2}$	7.8	1.7	0.089	-2.8	
	$1\frac{1}{2} \leftarrow \frac{1}{2}$	$\frac{1}{2}$	13.90 <sup>d</sup>	-1.0	0.086	-10.7	
$1\frac{1}{2} \leftarrow 1\frac{1}{2}$	$-1\frac{1}{2} \leftarrow -\frac{1}{2}$	$\frac{1}{2}$	19.49 <sup>d</sup>	-0.4	0.068	-7.7	
	$-1\frac{1}{2} \leftarrow -\frac{1}{2}$	$-\frac{1}{2}$	20.4	0.2	0.068	-5.2	
$\frac{1}{2} \leftarrow \frac{1}{2}$	$-\frac{1}{2} \leftarrow -\frac{1}{2}$	$\frac{1}{2}$	171.4	-6.3	0.021	-32.8	
	$-\frac{1}{2} \leftarrow \frac{1}{2}$	$-\frac{1}{2}$	175.5	-5.2	0.021	-32.8	
$3\frac{1}{2} \leftarrow 2\frac{1}{2}$	$-1\frac{1}{2} \leftarrow -\frac{1}{2}$	$\frac{1}{2}$	204.4	-5.6	0.033	-23.1	
	$-1\frac{1}{2} \leftarrow -\frac{1}{2}$	$-\frac{1}{2}$	244.3	-4.8	0.033	-23.3	
166.6 $\mu\text{m}$ spectrum $\nu_L = 1\,799\,139.3$ MHz $N = 2 \leftarrow 1$							
polarization ( $\pi$ )							
$1\frac{1}{2} \leftarrow 1\frac{1}{2}$	$-1\frac{1}{2} \leftarrow -1\frac{1}{2}$	$\frac{1}{2}$	21.08 <sup>d</sup>	1.2	0.156	15.5	
	$-1\frac{1}{2} \leftarrow -1\frac{1}{2}$	$-\frac{1}{2}$	25.72 <sup>d</sup>	0.7	0.161	15.6	
$\frac{1}{2} \leftarrow \frac{1}{2}$	$\frac{1}{2} \leftarrow \frac{1}{2}$	$\frac{1}{2}$	92.8 <sup>d</sup>	-5.4	0.055	-43.3	
	$\frac{1}{2} \leftarrow \frac{1}{2}$	$-\frac{1}{2}$	96.0	-4.8	0.055	-43.2	
$1\frac{1}{2} \leftarrow 1\frac{1}{2}$	$-\frac{1}{2} \leftarrow -\frac{1}{2}$	$\frac{1}{2}$	109.34 <sup>d</sup>	0.5	0.120	5.8	
	$-\frac{1}{2} \leftarrow -\frac{1}{2}$	$-\frac{1}{2}$	112.64 <sup>d</sup>	0.5	0.121	5.9	
$3\frac{1}{2} \leftarrow 2\frac{1}{2}$	$2\frac{1}{2} \leftarrow 2\frac{1}{2}$	$\frac{1}{2}$	191.1	-4.9	0.036	-22.9	
		$-\frac{1}{2}$	195.1	-3.4	0.036	-23.0	
$3\frac{1}{2} \leftarrow 2\frac{1}{2}$	$\frac{1}{2} \leftarrow \frac{1}{2}$	$\frac{1}{2}$	224.9	-6.2	0.023	-27.4	
		$-\frac{1}{2}$	228.7	-5.3	0.023	-27.3	
l polarization ( $\sigma$ )							
$1\frac{1}{2} \leftarrow 1\frac{1}{2}$	$-\frac{1}{2} \leftarrow -1\frac{1}{2}$	$\frac{1}{2}$	14.1	1.8	0.083	26.2	
		$-\frac{1}{2}$	18.5	0.4	0.079	26.4	
$1\frac{1}{2} \leftarrow 1\frac{1}{2}$	$\frac{1}{2} \leftarrow -\frac{1}{2}$	$\frac{1}{2}$	58.83 <sup>d</sup>	0.8	0.108	4.0	
		$-\frac{1}{2}$	66.5 <sup>c</sup>	1.1	0.108	4.0	
$\frac{1}{2} \leftarrow \frac{1}{2}$	$-\frac{1}{2} \leftarrow \frac{1}{2}$	$\frac{1}{2}$	156.6	-3.1	0.028	-33.3	
		$-\frac{1}{2}$	160.7	-3.5	0.028	-33.2	
$3\frac{1}{2} \leftarrow 2\frac{1}{2}$	$-\frac{1}{2} \leftarrow \frac{1}{2}$	$\frac{1}{2}$	175.7	-4.4	0.012	-24.7	
		$-\frac{1}{2}$	179.6	-3.1	0.012	-24.7	
$3\frac{1}{2} \leftarrow 2\frac{1}{2}$	$-1\frac{1}{2} \leftarrow -\frac{1}{2}$	$\frac{1}{2}$	218.9	-4.4	0.039	-22.4	
		$-\frac{1}{2}$	222.7	-3.5	0.039	-22.4	
110.7 $\mu\text{m}$ spectrum $\nu_L = 2\,707\,749.3$ MHz $N = 3 \leftarrow 2$							
polarization ( $\pi$ )							
$3\frac{1}{2} \leftarrow 3\frac{1}{2}$	$-3\frac{1}{2} \leftarrow -3\frac{1}{2}$	$\frac{1}{2}$	19.5	-0.6	0.040	19.8	
		$-\frac{1}{2}$	22.1	-0.9	0.041	19.8	
$3\frac{1}{2} \leftarrow 3\frac{1}{2}$	$-2\frac{1}{2} \leftarrow -2\frac{1}{2}$	$\frac{1}{2}$	20.2	-0.1	0.020	23.8	
		$-\frac{1}{2}$	23.1	0.0	0.022	23.6	
$3\frac{1}{2} \leftarrow 3\frac{1}{2}$	$1\frac{1}{2} \leftarrow 1\frac{1}{2}$	$\frac{1}{2}$	50.0	0.8	0.004	20.3	
		$-\frac{1}{2}$	54.4	0.1	0.006	20.9	
l polarization ( $\alpha$ ) $\sigma$							
$3\frac{1}{2} \leftarrow 3\frac{1}{2}$	$-2\frac{1}{2} \leftarrow -3\frac{1}{2}$	$\frac{1}{2}$	13.0	-1.9	0.011	31.5	
		$-\frac{1}{2}$	15.5	-0.8	0.010	30.7	
	$-1\frac{1}{2} \leftarrow -2\frac{1}{2}$	$\frac{1}{2}$	14.4	-1.2	0.018	31.1	
		$-\frac{1}{2}$	17.2	-1.8	0.022	30.3	
	$-\frac{1}{2} \leftarrow -1\frac{1}{2}$	$\frac{1}{2}$	16.6	-1.8	0.018	29.6	
		$-\frac{1}{2}$	19.8	-2.2	0.022	28.8	
	$\frac{1}{2} \leftarrow -\frac{1}{2}$	$\frac{1}{2}$	20.2	-3.0	0.022	26.9	
		$-\frac{1}{2}$	23.8	-2.6	0.023	26.2	
	$1\frac{1}{2} \leftarrow \frac{1}{2}$	$\frac{1}{2}$	26.9	0.7	0.017	22.7	
		$-\frac{1}{2}$	31.0	-0.9	0.021	22.4	
	$-2\frac{1}{2} \leftarrow -1\frac{1}{2}$	$\frac{1}{2}$	34.9	-1.2	0.020	20.5	
		$-\frac{1}{2}$	38.4	-1.9	0.019	20.5	
	$-1\frac{1}{2} \leftarrow -\frac{1}{2}$	$\frac{1}{2}$	37.0	-1.0	0.024	23.5	
		$-\frac{1}{2}$	40.9	-1.9	0.024	23.4	
$3\frac{1}{2} \leftarrow 3\frac{1}{2}$	$-3\frac{1}{2} \leftarrow -2\frac{1}{2}$	$\frac{1}{2}$	42.5	1.3	0.016	11.9	
	$-\frac{1}{2} \leftarrow \frac{1}{2}$	$\frac{1}{2}$	43.9	1.7	0.025	24.0	
		$-\frac{1}{2}$	48.0	2.6	0.026	24.0	
	$\frac{1}{2} \leftarrow 1\frac{1}{2}$	$\frac{1}{2}$	59.1	4.2	0.022	23.5	
		$-\frac{1}{2}$	63.7	3.5	0.023	23.8	
$2\frac{1}{2} \leftarrow 3\frac{1}{2}$	$-1\frac{1}{2} \leftarrow -2\frac{1}{2}$	$\frac{1}{2}$	98.7	9.9	0.008	42.0	
		$-\frac{1}{2}$	102.1	5.9	0.008	41.8	
	$-2\frac{1}{2} \leftarrow -3\frac{1}{2}$	$\frac{1}{2}$	105.6	6.3	0.006	23.0	

<sup>a</sup> Almost all the observed transitions obey the selection rule  $\Delta M_T = 0$ .

<sup>b</sup> Value calculated using the parameter values given in Table III.

<sup>c</sup> Overlapped line, given zero weight in the least-squares fit.

<sup>d</sup> Measurement refers to a Lamb dip, assigned a relative weight of 100 in the least-squares fit.

phenomenon which arises whenever the fine structure splittings are small (that is, comparable with the Zeeman energies).<sup>32</sup> It is particularly damaging for magnetic resonance experiments in which transitions are required to be both intense and tunable. Above a certain flux density, a given transition can be either intense but not tunable (electric dipole allowed,  $\Delta M_S = 0$ ) or weak and tunable (electric dipole forbidden,  $\Delta M_S = \pm 1$ ). For this reason, transitions were not observed above 0.5 T in the present work. The electron spin decoupling effects can be seen in Fig. 5 which shows the behavior of individual  $M_F$  levels of the  $N = 1$  rotational level of  $^4\Sigma^-$  CH as a function of applied magnetic field. The decoupling is marked by a strong curvature in the levels. In the high field limit, they behave as one of the four possible  $M_S$  states ( $M_S = \pm \frac{3}{2}, \pm \frac{1}{2}$ ). The diagram also shows that the proton nuclear spin is similarly decoupled but at very much lower flux densities ( $\sim 0.02$  T). Furthermore, there is an anticrossing between the two  $M_F = 0$  levels at about 0.16 T. The anticrossing is weak because it arises from nuclear hyperfine effects.

The assignments of individual spectra were based on the experimental Zeeman patterns. These comprise the observed flux densities, the relative intensities, the linewidths (in mT) and the sign of the tuning rate, the last being determined from the shift in the resonance on altering the length of the FIR laser cavity. A computer program was used to calculate the frequencies of individual  $M$  transitions as a function of applied magnetic field and the results were plotted as shown in Figs. 6 and 7. Such diagrams provided the key to the correct assignment. Although the magnitude of the transition frequency depends primarily on the rotational constant, the detailed behavior of the Zeeman components for a particular rotational transition depends more on the values adopted for

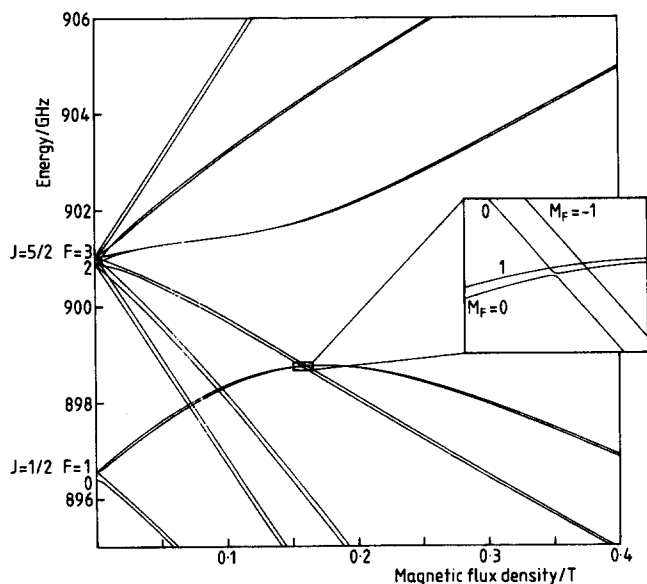


FIG. 5. Energy level diagram showing the dependence of individual  $M_F$  levels in the  $N = 1$  rotational level of CH in its  $a^4\Sigma^-$  state upon applied magnetic field. The proton nuclear spin is decoupled at very low flux densities ( $< 10$  mT) while the electron spin becomes decoupled above 0.25 T. A weak anticrossing of two  $M_F = 0$  levels is shown in expanded form on the right-hand side of the diagram.

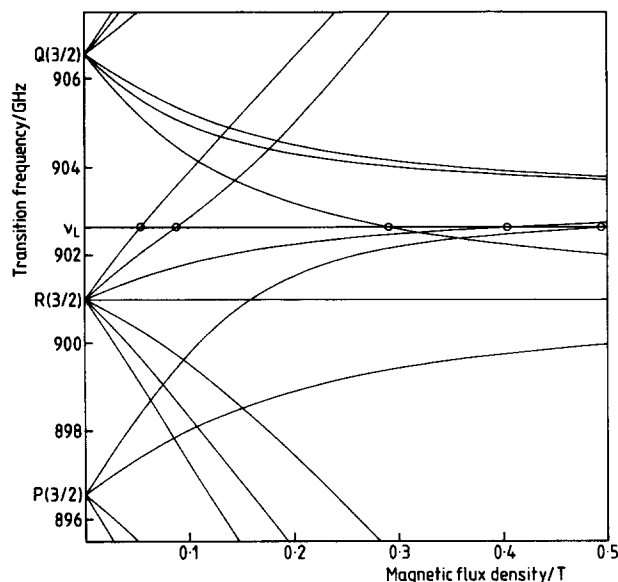


FIG. 6. Diagram showing the variation of  $\Delta M_J = \pm 1$  components of the  $N = 1 \rightarrow 0$  transition of CH in the  $v = 0$  level of the  $a^4\Sigma^-$  state with applied magnetic field. Proton hyperfine splittings are not shown. The resonances predicted for a laser frequency of 902.630 GHz are indicated by open circles. They correspond to the experimental spectrum recorded at  $332.1 \mu\text{m}$  which is shown in Fig. 2. The transitions which became less tunable as the field increases are those which retain their electric dipole intensity.

the fine structure parameters  $\lambda$  and  $\gamma$ . The predictions for a range of values for these two parameters were compared with the experimental spectra until a reasonable match was discovered. From this it was possible to make detailed assignments and thence to refine the molecular parameters to achieve the best fit. Figure 6 shows the magnetic field depend-

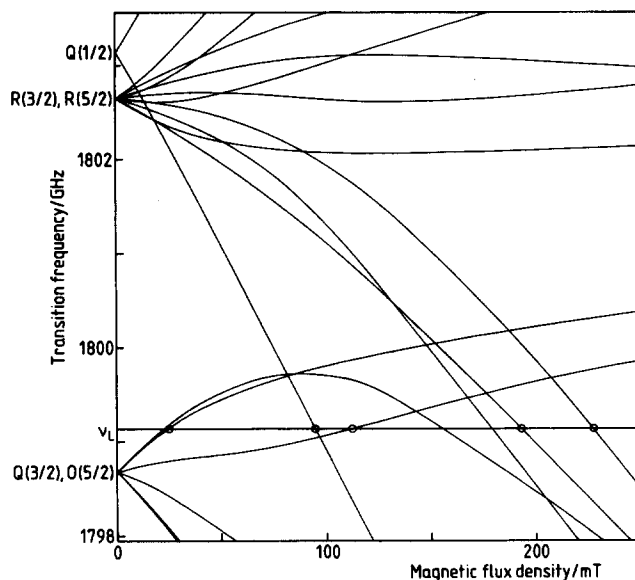


FIG. 7. Diagram showing the variation of individual  $\Delta M_J = 0$  components of the  $N = 2 \rightarrow 1$  transition of CH in the  $v = 0$  level of its  $a^4\Sigma^-$  state with applied magnetic field. Proton hyperfine splittings are not shown. The resonances predicted for a laser frequency of 1799.139 GHz are shown by open circles and correspond to the experimental spectrum recorded at  $166.6 \mu\text{m}$  shown in Fig. 3.

dence of the  $\Delta M_J = \pm 1$  Zeeman components of the  $N = 1 \leftarrow 0$  transition computed with the optimized parameters given in Table III. It provides the basis for the assignment of the spectrum recorded with the 332.1  $\mu\text{m}$  laser line in  $\sigma$  polarization, which is shown in Fig. 2. Figure 7 shows the similar diagram for the  $\Delta M_J = 0$  components of the  $N = 2 \leftarrow 1$  transition. The corresponding experimental spectrum in this case is that recorded with the 166.6  $\mu\text{m}$  laser line, shown in Fig. 3. The full details of the assignments made in this way are given in Table II. Almost all the transitions obey the nuclear spin selection rule  $\Delta M_I = 0$ , consistent with the ready decoupling of the nuclear spin.

When all the assignments had been made, the molecular parameters for CH in the  $a^4\Sigma^-$  state were determined by a least-squares procedure. The eigenvalues were calculated as described earlier and the parameter values adjusted to give the best fit. The basis set was truncated in the calculations at  $\Delta N = \pm 2$  without loss in accuracy. It was not possible to determine the electron spin  $g$  factor in the fit so it was constrained to the free electron value, 2.0023. Each experimental measurement was given the same weight (unity) in the fit except that the measurements of Lamb dips were considered to be an order of magnitude more precise and were weighted accordingly. The residuals obtained in the fit are given in Table II and the parameter values determined, together with their standard deviations, are given in Table III. The standard deviation of the fit, for a point of unit weight, is 1.4 MHz which is considered to be closer to the limit imposed by experimental error. Eight parameter values are determined in the fit, including the third order spin-rotation term  $\gamma_S$  and two proton hyperfine parameters  $b_F$  and  $c$ . These parameters are well determined by the data as can be judged from the relatively small values for the correlation coefficients  $\kappa_i$  which are also given in Table III.

## V. DISCUSSION

This paper describes the first observations and detailed characterization of CH in a quartet state. It is perhaps surprising that it has not been detected earlier through electronic transitions involving the  $a^4\Sigma^-$  state. However, *ab initio* calculations<sup>33</sup> suggest that such transitions will be very

TABLE III. Molecular parameters (in MHz) for CH in the  $\nu = 0$  level of the  $a^4\Sigma^-$  state determined in a fit of the LMR data.

Parameter	Value	Correlation $\kappa_i^a$
$B$	451 138.434(94) <sup>b</sup>	4.309
$D$	44.427(13)	4.477
$\lambda$	2 785.83(18)	2.110
$\gamma$	-1.74(12)	1.817
$\gamma_S$	0.154(93)	2.680
$b_F$	106.56(84)	1.294
$c$	56.6(11)	1.131
$g_S$	2.0023 <sup>c</sup>	fixed
$10^3 g_r$	-0.164(47)	1.340

<sup>a</sup> Correlation  $\kappa_i = (\chi^{-1})_{ii}$ , where  $\chi$  is the matrix of correlation coefficients.

<sup>b</sup> Values in parenthesis correspond to one standard deviation of the least squares fit in units of the last quoted digit.

<sup>c</sup> Parameter constrained to this value in the fit.

hard to detect, because they occur only weakly if at all in the vacuum ultraviolet region where it is difficult to work.

The various parameters for CH in the  $a^4\Sigma^-$  state which have been determined provide information about its structure. The principal parameter is the rotational constant  $B_0 = 451\,138.4\text{ MHz}$  or  $15.048\,36\text{ cm}^{-1}$ . This value was well predicted by the *ab initio* CI calculation of Lie *et al.*,<sup>20</sup> see Table IV, a result which considerably aided initial searches for rotational transitions in CH in its  $a^4\Sigma^-$  state. The  $B_0$  value allows the CH bond length to be determined for the first time. The vibrationally averaged bond length  $r_0$  is calculated to be 109.767 pm for the  $a^4\Sigma^-$  state, slightly shorter than the corresponding bond length for CH in its ground  $^2\Pi$  state of 113.029 pm. The quartic centrifugal distortion parameter  $D$  is also well determined and provides information on the harmonic force field. The value in Table III suggests a harmonic vibrational wave number of  $3033\text{ cm}^{-1}$ , in reasonably good agreement with the value of  $3160\text{ cm}^{-1}$  from the *ab initio* calculation.<sup>20</sup>

The spin-spin coupling constant  $\lambda$  has two major contributions,  $\lambda^{(1)}$  which is the direct spin-spin dipolar interaction and  $\lambda^{(2)}$  which describes the second order spin-orbit mixing of other electronic states:

$$\lambda = \lambda^{(1)} + \lambda^{(2)}. \quad (9)$$

The largest contribution to  $\lambda^{(2)}$  is likely to come from the admixture of the closest electronic state, namely the  $X^2\Pi$  state. If we assume that this state lies an amount  $\Delta = 6030\text{ cm}^{-1}$  below the  $a^4\Sigma^-$  state and that the atomic spin-orbit coupling constant for a single electron in a  $2p$  orbital on a carbon atom is  $\zeta = 27.5\text{ cm}^{-1}$ ,<sup>35</sup> we estimate that  $\lambda^{(2)} \approx \zeta^2 / (12\Delta) = 313\text{ MHz}$  or  $0.0105\text{ cm}^{-1}$ . The experimentally determined value of 2786 MHz for  $\lambda$  is much larger than this estimated second order contribution and therefore appears to arise predominantly from the direct dipolar coupling. The spin-rotation constant  $\gamma$  has an exceptionally small value of  $-1.74\text{ MHz}$ ; the value for the same parameter in the  $X^2\Pi$  state of CH is  $-771\text{ MHz}$ .<sup>16</sup> This suggests that the  $^4\Pi$  states of CH lie at very high energies<sup>33</sup> and are only weakly mixed with the  $a^4\Sigma^-$  state by spin-orbit coupling.

Two proton hyperfine parameters, the Fermi contact parameter  $b_F$  and the dipolar term  $c$ , have been determined. The former is positive and quite a bit larger than the corresponding parameter for CH in its  $X^2\Pi$  state ( $b_F = -57.7\text{ MHz}$ ), as expected from the single configuration wave function for the  $^4\Sigma^-$  state of  $|\sigma\pi^2\rangle$ .<sup>16</sup> Following our preliminary communication,<sup>19</sup> theoretical estimates of these hyperfine parameters were made by Veseth<sup>35</sup> and, more recently, by Engels *et al.*<sup>21</sup> Veseth's calculation is based

TABLE IV. Comparison of experimental and theoretical values for the parameters of CH in the  $\nu = 0$  level of the  $a^4\Sigma^-$  state.

Parameter	Experiment <sup>a</sup>	Theory	Reference
$B_0/\text{GHz}$	451.138	450.9	20
$D_0/\text{MHz}$	44.43	41.7	20
$b_F/\text{MHz}$	106.6	101.4	35
$c/\text{MHz}$	56.6	57.6	35

<sup>a</sup> Values taken from the present work, Table III.

on many-body perturbation treatment of configuration interaction wave functions<sup>36</sup> and gives remarkably good agreement with the experimental values, as can be seen in Table IV. The values of Engels *et al.* are very similar; these authors give the <sup>13</sup>C hyperfine parameters also.

Much experimental work remains to be done on the CH radical in its  $a^4\Sigma^-$  state. It would be interesting to study the molecule in excited vibrational levels and it is likely that rotational transitions in the  $v = 1$  level could be detected by far infrared LMR. Because of the expected large change in  $B$  with  $v$ ,<sup>20</sup> the transitions will occur at frequencies well below those reported in this paper. The same information could also be obtained by detecting vibration-rotation transitions in the infrared; our estimate of the harmonic wave number will be useful in this connection. It would also be worthwhile to study <sup>13</sup>CH in the  $a^4\Sigma^-$  state, with the objective of mea-

suring the <sup>13</sup>C hyperfine parameters and so characterizing the wave function in the region of the carbon nucleus. Finally, there remains the possibility of detecting electronic transitions between the quartet states of CH in the vacuum ultraviolet. The development of tunable laser sources in this region of the spectrum increases the chances of making such observations in absorption.

## ACKNOWLEDGMENTS

Work supported by the U.S. Government, not subject to copyright. Supported in part by NASA Contract No. W,15-047. We thank Dr. Leif Veseth for sending us the results of his calculations on the proton hyperfine structure of CH in its  $a^4\Sigma^-$  state. We are also very grateful to the Carl Duisberg Stiftung, Leverkusen for the support of T. N.

## APPENDIX

Explicit algebraic expressions for the third order spin rotation term in a case (b) basis set can be derived from Eq. (8). Using the expressions for the third rank 6- $j$  symbols given by Sato<sup>37</sup> we obtain:

$$\begin{aligned} \langle NSJ | H_{sr}^{(3)} | NSJ \rangle &= -\gamma_s [(S+J-N)(S+J-N-1)(S+J-N-2)(N+J-S)(N+J-S-1)(N+J-S-2) \\ &\quad - 9(S+J-N)(S+J-N-1)(N+J-S)(N+J-S-1)(N+S-J)(N+S+J+2) \\ &\quad + 9(S+J-N)(N+J-S)(N+S-J)(N+S-J-1)(N+S+J+3)(N+S+J+2) \\ &\quad - (N+S-J)(N+S-J-1)(N+S-J-2)(N+S+J+4)(N+S+J+3) \\ &\quad \times (N+S+J+2)] / [16(2N-1)(2N+3)], \end{aligned} \quad (A1)$$

$$\begin{aligned} \langle N+2SJ | H_{sr}^{(3)} | NSJ \rangle &= \frac{5}{16}\gamma_s [(S+J-N)(S+J-N-1)(N+J-S+2)(N+J-S+1) \\ &\quad \times (N+S-J+2)(N+S-J+1)(N+S+J+3)(N+S+J+2)]^{1/2} [(S+J-N-2) \\ &\quad \times (N+J-S) - (N+S-J)(N+S+J+4)]^{1/2} / [(2N+1)(2N+3)^2(2N+5)]^{1/2}. \end{aligned} \quad (A2)$$

For the specific case of a molecule in a  $^4\Sigma$  state, the matrix elements are

Diagonal elements  $\langle NJ | H | NJ \rangle$

$F_1(J = N + \frac{3}{2})$ :

$$BN(N+1) - DN^2(N+1)^2 - \lambda \frac{2N}{(2N+3)} + \frac{1}{2}\gamma N - \frac{3}{2}\gamma_s \frac{N(N-1)}{(2N+3)}, \quad (A3)$$

$F_2(J = N + \frac{1}{2})$ :

$$BN(N+1) - DN^2(N+1)^2 + \lambda \frac{2(N+3)}{(2N+3)} + \frac{1}{2}\gamma(N-3) + \frac{3}{2}\gamma_s \frac{(N+2)(N-1)}{(2N+3)}, \quad (A4)$$

$F_3(J = N - \frac{1}{2})$ :

$$BN(N+1) - DN^2(N+1)^2 + \lambda \frac{2(N-2)}{(2N-1)} - \frac{1}{2}\gamma(N+4) - \frac{3}{2}\gamma_s \frac{(N+2)(N-1)}{(2N-1)}, \quad (A5)$$

$F_4(J = N - \frac{3}{2})$ :

$$BN(N+1) - DN^2(N+1)^2 - \lambda \frac{2(N+1)}{(2N-1)} - \frac{3}{2}\gamma(N+1) + \frac{1}{2}\gamma_s \frac{(N+2)(N+1)}{(2N-1)}. \quad (A6)$$

Off-diagonal elements  $\langle N+2J | H | NJ \rangle$

$$\langle N+2, J = N + \frac{3}{2} | H | N, J = N + \frac{3}{2} \rangle = [2\lambda + \frac{3}{2}\gamma_s N] [3(N+1)(N+3)]^{1/2} / (2N+3), \quad (A7)$$

$$\langle N+2, J = N + \frac{1}{2} | H | N, J = N + \frac{1}{2} \rangle = [2\lambda - \frac{3}{2}\gamma_s(N+3)] [3N(N+2)]^{1/2} / (2N+3). \quad (A8)$$

- <sup>1</sup>J. E. Butler, J. W. Flemming, L. P. Goss, and M. C. Lin, *Chem. Phys.* **56**, 355 (1981).
- <sup>2</sup>K. D. Bayes, *Chem. Phys. Lett.* **152**, 424 (1988).
- <sup>3</sup>C. E. Moore and H. P. Broida, *J. Res. Natl. Bur. Stand. Sect. A* **63**, 19 (1959).
- <sup>4</sup>O. E. H. Rydbeck, J. Ellder and W. M. Irvine, *Nature* **246**, 466 (1973).
- <sup>5</sup>B. E. Turner and B. Zuckerman, *Astrophys. J. Lett.* **187**, L59 (1974).
- <sup>6</sup>T. Heulinger, Dissertation, University of Lund, Sweden, 1918.
- <sup>7</sup>E. Hultén, *Z. Phys.* **11**, 284 (1922).
- <sup>8</sup>A. Kratzev, *Z. Phys.* **23**, 298 (1924).
- <sup>9</sup>R. S. Mulliken, *Phys. Rev.* **30**, 785 (1927).
- <sup>10</sup>L. Gerö, *Z. Phys.* **117**, 709 (1941).
- <sup>11</sup>G. Herzberg and J. W. C. Johns, *Astrophys. J.* **158**, 399 (1969).
- <sup>12</sup>K. M. Evenson, H. E. Radford, and M. M. Moran, *Appl. Phys. Lett.* **18**, 426 (1971).
- <sup>13</sup>J. T. Hougen, J. A. Mucha, D. A. Jennings, and K. M. Evenson, *J. Mol. Spectrosc.* **72**, 463 (1978).
- <sup>14</sup>J. M. Brown and K. M. Evenson, *J. Mol. Spectrosc.* **98**, 392 (1986).
- <sup>15</sup>S. A. Davidson, K. M. Evenson, and J. M. Brown (in preparation).
- <sup>16</sup>C. R. Brazier and J. M. Brown, *Can. J. Phys.* **62**, 1563 (1984).
- <sup>17</sup>M. Bogey, C. Demuyneck, and J.-L. Destombes, *Chem. Phys. Lett.* **100**, 105 (1983).
- <sup>18</sup>K. G. Lubic and T. Amano, *J. Chem. Phys.* **81**, 1655 (1984).
- <sup>19</sup>T. Nelis, J. M. Brown, and K. M. Evenson, *J. Chem. Phys.* **88**, 2087 (1988).
- <sup>20</sup>G. C. Lie, J. Hinze, and B. Liu, *J. Chem. Phys.* **57**, 625 (1972).
- <sup>21</sup>B. Engels, S. D. Peyerimhoff, S. P. Karna, and F. Grein, *Chem. Phys. Lett.* **152**, 397 (1988).
- <sup>22</sup>A. Kasdan, E. Herbst, and W. C. Lineberger, *Chem. Phys. Lett.* **31**, 78 (1975).
- <sup>23</sup>T. J. Sears, P. R. Bunker, A. R. W. McKellar, K. M. Evenson, D. A. Jennings, and J. M. Brown, *J. Chem. Phys.* **77**, 5348 (1982).
- <sup>24</sup>M. Inguscio, G. Moruzzi, K. M. Evenson, and D. A. Jennings, *J. Appl. Phys.* **60**, R161 (1986).
- <sup>25</sup>D. K. Russell and H. E. Radford, *J. Chem. Phys.* **72**, 2750 (1980).
- <sup>26</sup>J. T. Hougen, *Can. J. Phys.* **40**, 598 (1962).
- <sup>27</sup>J. M. Brown and D. J. Milton, *Mol. Phys.* **31**, 409 (1976).
- <sup>28</sup>A. S.-C. Cheung, R. C. Hansen, and A. J. Merer, *J. Mol. Spectrosc.* **91**, 165 (1982).
- <sup>29</sup>A. R. Edmonds, *Angular Momentum in Quantum Mechanics* (Princeton University, Princeton, 1960).
- <sup>30</sup>J. M. Brown, A. S.-C. Cheung, and A. J. Merer, *J. Mol. Spectrosc.* **124**, 464 (1987).
- <sup>31</sup>G. Herzberg, *Molecular Spectra and Structure I. Diatomic Molecules* (Van Nostrand, New York, 1950).
- <sup>32</sup>B. J. Boland, J. M. Brown, and A. Carrington, *Proc. R. Soc. London Ser. A* **360**, 507 (1978).
- <sup>33</sup>H. P. D. Liu and G. Verhaegen, *J. Chem. Phys.* **53**, 735 (1970).
- <sup>34</sup>A. Carrington and A. D. McLachlan, *Introduction to Magnetic Resonance* (Harper and Row, New York, 1962), p.138.
- <sup>35</sup>L. Veseth (private communication, Sept. 1987).
- <sup>36</sup>P. Kristiansen and L. Veseth, *J. Chem. Phys.* **84**, 2711 (1986).
- <sup>37</sup>M. Sato, *Prog. Theor. Phys.* **13**, 405 (1955).